

---

## Application of derivative spectroscopy method to photoluminescence in ZnS:Mn nanocrystals

Kovalenko A. V., Plakhtiy E. G. and Vovk S. M.

Oles Honchar Dnipro National University, 72 Gagarin Ave., 49010 Dnipro, Ukraine

**Received:** 13.03.2018

**Abstract.** An improved derivative spectroscopy method is proposed to resolve elementary bands in experimental photoluminescence spectra with high accuracy. The main procedures of analysis and calculations in the frame of this method are described. The method is tested on a synthetic photoluminescence spectrum consisting of five elementary Gaussian bands. The resolution of our method applied to overlapped Gaussian bands is estimated depending on their bandwidths. The photoluminescence spectrum of ZnS:Mn nanocrystals obtained with a self-propagating high-temperature synthesis is analyzed, using our derivative spectroscopy method. Six photoluminescence bands are found, with their peaks located at the wavelengths equal to 540, 559, 579, 600, 620 and 643 nm.

**Keywords:** derivative spectroscopy method, photoluminescence, elementary emission bands, ZnS:Mn nanocrystals.

**PACS:** 78.55

**UDC:** 538.958

### 1. Introduction

Up to now, an Alentsev–Fock method [1] is most often used in decomposing experimental photoluminescence (PL) spectra into individual elementary bands. It is based on the fact that, when the excitation conditions are changed, the PL spectrum changes its shape as a result of changing intensities of elementary emission bands associated with different PL centres. Then the analysis of the PL spectra obtained under different excitation conditions and the appropriate calculations make it possible to reveal the elementary bands, estimate their intensities, locations of the emission peaks, and the half-width of these bands. However, the Alentsev–Fock method has some disadvantages: (i) the corresponding experimental PL spectra should differ significantly from each other in both the shapes and the widths of the bands and, (ii) the same PL centres should take part [2] in the radiation process under different excitation conditions.

The other efficient approach for identifying individual PL bands is a  $\lambda$ -modulation method, which allows detecting experimentally very weak elementary PL bands. As a rule, this implies recording of the first derivatives and, sometimes, of the second derivative of the optical signal. An important drawback of the method is its low noise immunity. To overcome the problem, one must use complex and expensive equipment [3].

There is also a number of software packages, e.g. Origin [4], which enable selecting a priori a certain number of elementary Gaussian components and then decomposing a given PL spectrum into these components. Although the calculated spectrum becomes closer to the real one with increasing number of elementary bands in the decomposition, this computer modelling can have little in common with the real physical processes. In other words, sometimes the individual emission bands thus obtained could not be associated with the real PL centres.

Another experimental technique used to resolve PL spectra and find the parameters of their elementary bands is represented by a derivative spectroscopy method (DSM) [5]. Its application requires neither numerous experiments nor expensive equipment. For these reasons, the DSM has become widely used when quantifying chemical compositions of medical preparations [6] and quality of food [7], analyzing uranium [8] and hydrogen [9] absorbance spectra in radioastrophysical studies, etc. The basis of the DSM is calculation of spectral derivatives of given orders in an experimental spectrum and matching among these derivatives and the parameters of elementary bands. Unlike the  $\lambda$ -modulation method where the spectral derivatives are obtained by means of experimental techniques, in the frame of the DSM one gets the derivatives using purely analytical processing of the data measured. Note that, in the both cases, the parameters of individual bands are determined from the data for a single experimental PL spectrum. In spite of the above advantages, the DSM reveals shortcomings, too. Usually, the analysis must be restricted to derivatives of the orders ranging from two to four, due to notable noises appearing for higher-order derivatives. As a result, the canonical version of the DSM detects the spectral positions of elemental PL bands with high enough precision, although the errors for their half-widths are essentially higher (up to  $\sim 100\%$ ).

In the present work we report an improved version of the DSM, approve it on the example of synthetic PL spectrum, and find the parameters of individual bands in the emission PL spectrum of ZnS:Mn nanocrystals, using our method.

## 2. Results and discussion

### 2.1. Bases of improved DSM

In general, application of the DSM method can be divided into the following stages: (1) experimental measurements of a PL spectrum; (2) elucidation of the nature and the levels of measurement noises, and smoothing the spectrum; (3) calculations of derivatives of the PL spectrum and derivation, on this basis, of the data concerned with the number of individual bands, as well as their intensities, locations and half-widths; (4) interpretation of the results. In this study, we focus mainly on the stage 3 of the DSM as its central point, thus considering that the problems described by the stages 1 and 2 have already been resolved.

As stressed above, the common version of the DSM deals with the second-, third- and fourth-order derivatives of the spectrum, basing on the assumptions that (i) the shape of its elementary components is described by the Gaussian function [9] and (ii) all of the derivatives are sufficiently smooth. While the first assumption is standard and a priori valid in the analysis of spectra of various origins, the second assumption remains justified only in case of the lowest-order derivatives. To obtain valuable additional information from the analysis of higher-order derivatives, one has to smooth the experimental spectrum and its derivatives. For this aim, one can apply a Tikhonov regularization method [10] to the solution of the corresponding linear integral equation with anti-differentiation operator [11]. As a result, the following simple relations must be satisfied at the wavelength points  $\lambda_{\max}$  where the peaks of the elementary spectral components are located:

$$I(\lambda) > \varepsilon, \quad d^2I(\lambda)/d\lambda^2 < 0, \quad d^3I(\lambda)/d\lambda^3 = 0, \quad d^4I(\lambda)/d\lambda^4 > 0, \quad (1)$$

where  $I(\lambda)$  is the spectral emission intensity and  $\varepsilon$  the threshold below which the experimental intensity data are not analyzed.

Hence, in general the technique consists in selecting the wavelength region ‘useful’ for the further analysis (see the first condition in Eqs. (1)), and searching for the  $\lambda = \lambda_{\max}$  points within

the selected region, where the last three conditions in Eqs. (1) are satisfied. These  $\lambda_{\max}$ 's can be used as estimates of the positions of elementary spectral components, and the number of actual spectral component is equal to the number of  $\lambda_{\max}$ 's that satisfy Eqs. (1). At the same time, the bandwidth of every elementary component, which has the Gaussian shape, can be evaluated by dividing the second-derivative by the fourth derivative taken at the maximum points. A subsequent use of the least-squares techniques allows one to estimate the amplitudes of the elementary spectral components.

Let us have two Gaussian curves  $I(\lambda) = I_0 \exp\left[-(\lambda - \lambda_{\max})^2 / (2\sigma^2)\right]$  with different locations  $\lambda_{\max}$  of their peaks, standard deviations  $\sigma$  that differ less than two times and identical (in practice – close) amplitudes  $I_0$ . Our numerical simulations of the problem of resolving the two Gaussian curves have shown that, according to the Rayleigh criterion, the ‘visual’ resolution of these curves occurs under the condition  $\Delta\lambda \geq 2.2\sigma$ , where  $\Delta\lambda$  is the distance between the curve peaks and  $\sigma$  is the larger standard deviation. The DSM based on the second-, third- and fourth-order derivatives provides a much higher resolution given by the condition  $\Delta\lambda \geq 1.5\sigma$ . However, the elementary components in many PL spectra usually have even greater overlaps. Therefore, the latter condition can appear to be insufficient. Elimination of this disadvantage is possible by increasing the order of derivatives used in the analysis.

Of course, increase in the order of derivatives within the DSM improves the condition of resolution of the Gaussian curves. For instance, we obtain the inequalities  $\Delta\lambda \geq 1.3\sigma$  in case of the fourth-, fifth- and sixth-order derivatives,  $\Delta\lambda \geq 1.1\sigma$  with the sixth-, seventh- and eighth-order derivatives, and even  $\Delta\lambda \geq \sigma$  with the eighth-, ninth- and tenth-order derivatives. However, the increase in the order of derivatives is limited since, even with high-quality smoothing of the data with the Tikhonov’s regularization technique, the errors of estimating the positions of Gaussian curves increases too much. In addition, there arise the errors of estimations of the number of peaks, due to appearance of additional false peaks.

In our numerical simulations, we have taken the noise  $\varepsilon$  to be close to its typical experimental values. Then the condition  $\varepsilon \approx 0.1I_{\max}$  holds true. We have found that an acceptable level of the accuracy is achieved if the sixth-, seventh- and eighth-order derivatives are employed. At the peak points of the elementary spectral components, the following formulae are satisfied:

$$I(\lambda) > \varepsilon, \quad d^6 I(\lambda) / d\lambda^6 < 0, \quad d^7 I(\lambda) / d\lambda^7 = 0, \quad d^8 I(\lambda) / d\lambda^8 > 0. \quad (2)$$

Then the  $\lambda_{\max}$  values satisfying Eqs. (2) can be used as an estimate of locations of the peaks of elementary components, whereas the number of  $\lambda_{\max}$ 's gives the number of elementary bands in

the PL spectrum. Finally, the relation  $\sigma = \sqrt{-7 \frac{d^6 I(\lambda) / d\lambda^6}{d^8 I(\lambda) / d\lambda^8}}$  has been obtained at the points of maxima of the elementary components, which allows estimating the standard deviation.

Since the  $\lambda_{\max}$  values and the parameters of elementary components of the PL spectrum usually contain errors due to measurement noises and computational errors, it will be expedient to refine still further the corresponding results. In the present study, this refinement has been carried out using the least-squares method, with the constraints that both the solution and the residual must be positive. An iterative scheme of coordinate descent technique has been used for its implementation, with sequential clarification of the parameter values for the Gaussian spectral components.

## 2.2. Application to synthetic spectrum

To demonstrate the potential of our DSM version, a non-elementary spectrum has been synthesized and analyzed. The spectrum consists of five elementary Gaussian bands with different positions ( $\lambda_{\max}$ ) of the peaks, standard deviations ( $\sigma$ ) and amplitudes ( $I_0$ ) (see Fig. 1a and Table 1). Fig. 1b displays the results of solving the inverse problem, i.e. decomposing the synthesized spectrum into its elementary Gaussian components, determining the individual bands (curves 1–5), and plotting their sum (curve 7) for estimating discrepancy with the initial spectrum (curve 6). The inverse problem has been solved with the aid of the DSM, basing on the analysis of the corresponding derivatives (see Fig. 2). The curves 6 and 7 in Fig. 1b coincide almost completely, while the parameters found during solving the inverse problem deviate only slightly from the parameters of the elementary bands introduced at the initial stage of spectrum synthesis (see Table 1). This implies high efficiency of our method.

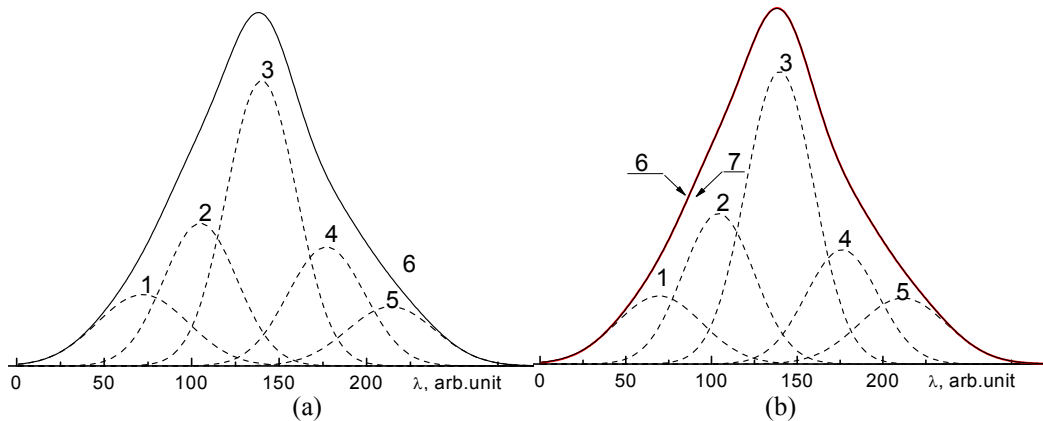


**Fig. 1.** Synthetic PL spectrum (curve 6) consisting of five (curves 1–5) elementary Gaussian bands (a) and decomposition of this spectrum (curve 6) into five individual bands (curves 1–5), using the DSM (b). Curve 7 in panel (b) corresponds to the sum of elementary bands found in the DSM analysis.

**Table 1.** Parameters of the initial and calculated Gaussian bands that constitute a synthetic PL spectrum displayed in Fig. 1.

№	Parameters of the initial Gaussian bands, arb. unit			Parameters of the calculated Gaussian bands, arb. unit			Deviations, %		
	$\lambda_{\max}$	$\sigma$	$I_0$	$\lambda_{\max}$	$\sigma$	$I_0$	$\lambda_{\max}$	$\sigma$	$I_0$
1	72	26	600	69.5	24.9	568.7	3.5	4.2	5.2
2	105	21	1200	104.1	20.8	1258.2	0.9	1.0	4.9
3	140	20	2400	139.9	19.9	2447.2	0.1	0.5	2.0
4	177	22	1000	176.3	21.1	954.9	0.4	4.1	4.5
5	214	25	500	211.6	25.5	551.8	1.1	2.0	10.4

## 2.3. Application to ZnS:Mn

In this subsection we analyze, using the DSM, the PL spectrum of ZnS:Mn nanocrystals. These nanocrystals have been obtained with a self-propagating high-temperature synthesis. The compound  $\text{Mn}(\text{NO}_3)_2$  in the amount of  $10^{-2}$  g/g has been added to the charge of zinc sulphide nanocrystals doped with manganese ions. The PL spectrum of the nanocrystals is shown in Fig. 3a. Below we analyze and compared it with the PL spectrum of ZnS:Mn single crystals, for which the parameters of the elementary Gaussian bands have been determined using the Alentsev–Fock method [12]. As reported in Ref. [12], the experimental PL spectrum of the ZnS:Mn nanocrystals

consists of five elementary bands (see Fig. 3a and Table 2). The sum of these bands agrees fairly well with the experimental PL spectrum (see curves 7 and 8 in Fig. 3a). Further on, we discard any detailed discussion of the nature of emitting centres associated with the above elementary PL bands (see Ref. [12]). In brief, all of these bands are associated with intra-centre emitting transitions occurring in  $\text{Mn}^{2+}$  ions placed in different local environments. In particular, the band at  $\lambda_{\text{max}2} = 557 \text{ nm}$  is associated with the  $\text{Mn}^{2+}$  ions located in interstitial sites of tetrahedrons of the cubic lattice,  $\lambda_{\text{max}3} = 578 \text{ nm}$  refers to  $\text{Mn}^{2+}$  located near deficient places in the lattice,  $\lambda_{\text{max}4} = 600 \text{ nm}$  is due to  $\text{Mn}^{2+}$  embedded in octahedral interstitial sites,  $\lambda_{\text{max}5} = 616 \text{ nm}$  corresponds to  $\text{Mn}^{2+}$  surrounded by oxygen atoms, and  $\lambda_{\text{max}6} = 637 \text{ nm}$  is linked with  $\text{Mn}^{2+}$  concentrated in  $\alpha\text{-MnS}$  phase.

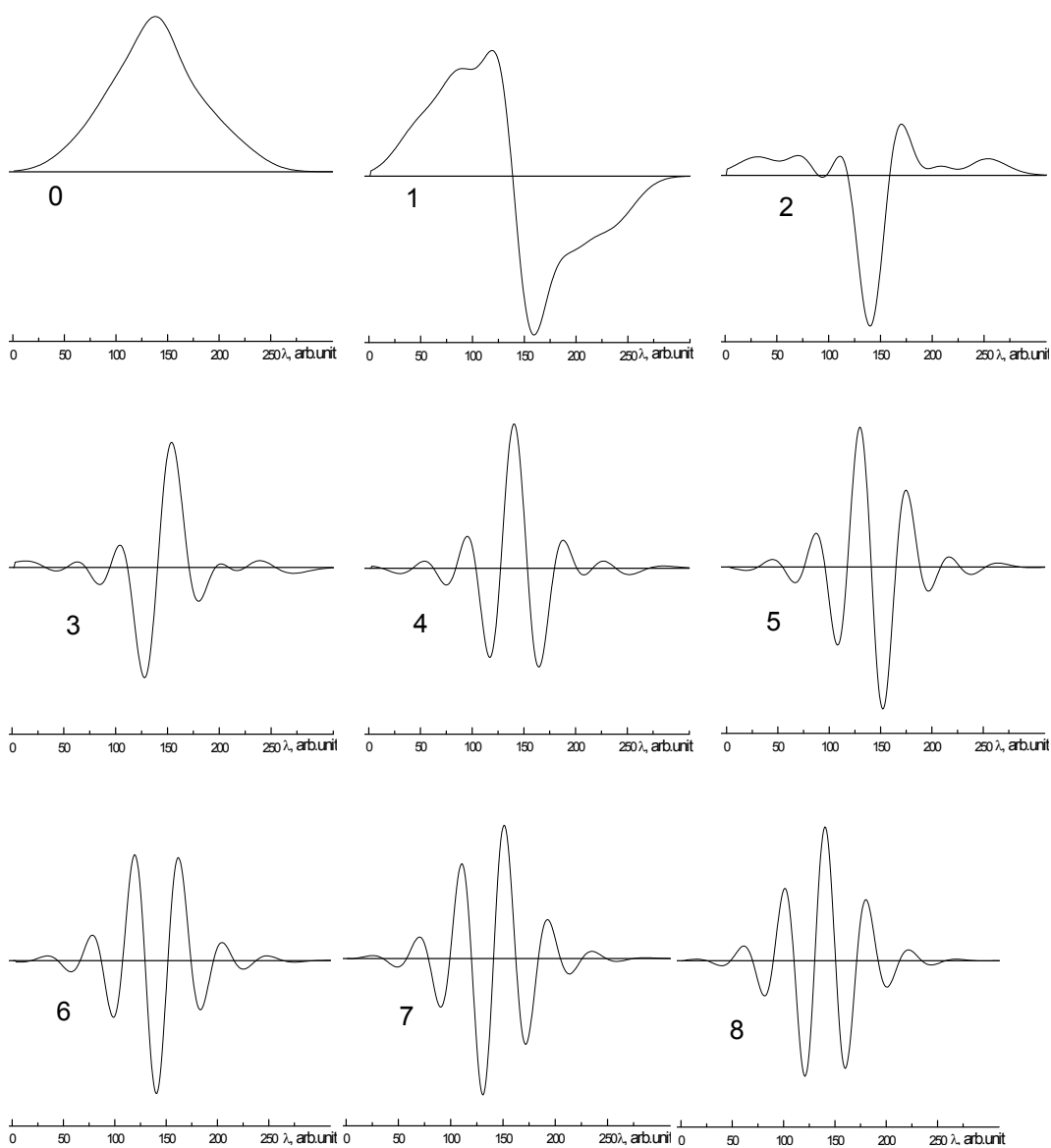


**Fig. 2.** Synthetic PL spectrum (curve 0) and its derivatives of the orders from one to eight (curves 1–8, respectively).

Like in the case of synthetic example spectrum, the PL spectrum of ZnS:Mn nanocrystals has been analyzed with the improved DSM, using the same threshold  $\varepsilon = 0.1I_{\max}$  as before. Six elementary Gaussian bands can be identified, as seen from Fig. 3b and Table 2. The positions of five of them, namely the Gaussian bands with the numbers 2–6 in Fig. 3b, either coincide completely with the elementary Gaussian-band positions  $\lambda_{\max}$  found previously – or correlate well with them, with the discrepancy values being in the range 1–6 nm (see Fig. 3a and Table 2).

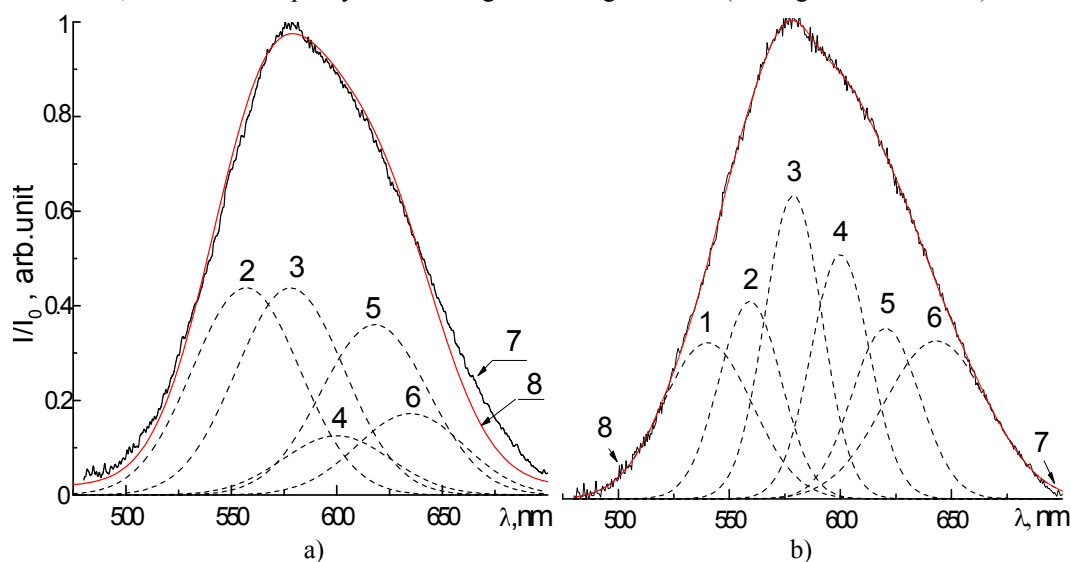


**Fig. 3.** Decompositions of the PL spectrum of ZnS:Mn nanocrystals into elementary Gaussian bands, as obtained using the Alentsev-Fock method [12] (panel a) and the DSM (panel b): curves 1–6 – elementary PL bands; curve 7 – experimental PL spectrum, and curve 8 – sum of the elementary PL bands.

**Table 2.** Parameters of elementary bands of the PL spectrum of ZnS:Mn nanocrystals, as obtained in Ref. [12] and in the present study.

№	Parameters of elementary bands according to Ref. [12]			Parameters of elementary bands obtained using our DSM			Deviations, %		
	$\lambda_{\max}$ , nm	$\sigma$ , nm	$I_0$ , a.u.	$\lambda_{\max}$ , nm	$\sigma$ , nm	$I_0$ , a.u.	$\lambda_{\max}$ , nm	$\sigma$ , nm	$I_0$ , a.u.
1	–	–	–	540	20.4	0.323	–	–	–
2	557	24.6	0.438	559	14	0.408	0.4	43.1	6.9
3	578	24.6	0.438	579	12.8	0.637	0.2	48.0	45.4
4	600	24.6	0.125	600	13.2	0.512	0	46.3	309.6
5	616	24.6	0.36	620	15.3	0.354	0.7	37.8	1.7
6	637	24.6	0.17	643	23.4	0.341	0.9	4.9	100.6

The sixth elementary PL band located at  $\lambda_{\max 1} = 540$  nm has not been revealed in the previous studies performed using the Alentsev–Fock method. After taking it into account, the resulting spectral curve coincides almost completely with the experimental PL spectrum (cf. curves 7 and 8 in Fig. 3b). This fact testifies a high accuracy of decomposition of the PL spectrum into individual Gaussian bands. It should be noted that a PL band centred in a close wavelength region,  $\lambda_{\max} = 530$ – $535$  nm, has earlier been observed for ZnS:Mn crystals [13]. It has been associated with isolated sulphur vacancies or uncontrolled copper in a doped material. We emphasize also that an individual PL band at  $\lambda_{\max} = 530$  nm has been observed in ZnS:Mn nanocrystals [12] obtained with the same self-propagating high-temperature synthesis and doped with manganese ions in case when  $\text{MnCl}_2$  is added to the charge.

At present, the nature of the elementary PL band located near 540 nm still remains unclear and needs its further investigations. Instead, we would pay attention to the other side of the issue. As seen from the examples of PL spectra illustrated above, the DSM evidently reveals a high resolution that allows for detecting the individual PL bands of relatively low intensities. In particular, it provides the decomposition of experimental PL spectrum for the ZnS:Mn nanocrystals into the individual bands, of which sum coincides with the experimental PL curve throughout all the contour. Notice that the average mean-squares error that quantifies the discrepancy between theory and experiment decreases by almost 30 times, when compared with the method Alentsev–Fock (cf. the curves 7 and 8 in Fig. 3a and Fig. 3b). This is a direct consequence of our improvement of the DSM.

### 3. Conclusion

The results obtained in the present work demonstrate that a properly improved version of the DSM can identify the elementary bands of very low intensities in the experimental PL spectra. Moreover, it enables reliable evaluation of their locations, half-widths and amplitudes. Basing on the results of our numerical simulations, we have found that the analysis of derivatives of the experimental PL spectra from the first to eighth orders ensures an acceptable accuracy of estimations of the elemental-band parameters. The individual bands can be resolved when their overlapping is as significant as  $(1.1\div 1.5)\sigma$ , where  $\sigma$  is the standard deviation for the Gaussian bands. As a principled example, we have analyzed, using the DSM, the PL spectra of the ZnS:Mn nanocrystals obtained with the self-propagating high-temperature synthesis. Six elementary PL bands are isolated, with the peak wavelengths  $\lambda_{\max}$  being equal to 540, 559, 579, 600, 620 and 643 nm. The exact nature of the centres responsible for these PL bands will be a subject of our forthcoming studies.

### References

1. Fock M V, 1972. Division of complex spectra on individual bands by means of generalized method of Alentsev. *Luminescence and Linear Optics*. **59**: 3–24.
2. Nekrasov A A, Ivanov V F and Vannikov A V, 2001. Effect of pH on the structure of absorption spectra of highly protonated polyaniline analyzed by the Alentsev–Fock method. *Electrochim. Acta*. **46**: 4051–4056.
3. Slyotov M M, Gavaleshko O S and Kinzerska O V, 2017. Preparation and luminescent properties of  $\alpha$ -ZnSe heterolayers with surface nanostructure. *J. Nano Electron. Phys.* **9**: 5046-1–5046-3.
4. OriginPro 9.1. OriginLab Corporation, One Roundhouse Plaza, suite 303, Northampton, MA 01060, United States. 1800-969-7720.
5. Talsky G. *Derivative spectroscopy: low and higher order*. Weinheim, Basel, Cambridge, New York, Tokyo: VCH Publishers (1994).
6. Joshi P R, Parmar S J and Patel B A, 2013. Spectrophotometric simultaneous determination of salbutamol sulfate and ketotifen fumarate in combined tablet dosage form by first-order derivative spectroscopy method. *Int. J. Spectrosc.* **2013**: 1–6.
7. Magwaza L S, Opara U L, Nieuwoudt H, Cronje P J, Saeys W and Nicolai B. NIR spectroscopy applications for internal and external quality analysis of citrus fruit – a review. *Food Bioproc. Technol.* **5**: 425–444.
8. El-Sayed A A and Hamed M M, 2006. Direct determination of U (VI) in TBP-kerosene extracts using first derivative ultraviolet spectroscopy. *J. Radioanalyt. Nucl. Chem.* **270**: 629–635.

9. Lindner R R, Vera-Ciro C, Murray C E, Stanimirović S, Babler B, Heiles C and Dickey J, 2015. Autonomous Gaussian decomposition. *Astronom. J.* **149**: 138–149.
10. Knowles I and Renka R J, 2014. Methods for numerical differentiation of noisy data. *Electron. J. Differ. Equations.* **21**: 235–246.
11. Vovk S M, 2017. Method for numerical differentiation of noisy data with outliers. *Radio Electron., Comp. Sci., Control.* **3**: 44–52.
12. Bulanyi M F, Kovalenko A V, Morozov A S and Khmelenko O V, 2017. Obtaining of nanocrystals ZnS:Mn by means of self-propagating high-temperature synthesis. *J. Nano Electron. Phys.* **9**: 2007-1–2007-4.
13. Kumar S S, Khadar M A, and Nair K G M, 2011. Analysis of the effect of annealing on the photoluminescence spectra of Cu<sup>+</sup> ion implanted ZnS nanoparticles. *J. Lumin.* **131**: 786–789.

---

Kovalenko A. V., Plakhtiy E. G. and Vovk S. M. 2018. Application of derivative spectroscopy method to photoluminescence in ZnS:Mn nanocrystals. *Ukr.J.Phys.Opt.* **19**: 133 – 140. doi: 10.3116/16091833/19/3/133/2018

*Анотація.* Запропоновано вдосконалений метод похідної спектроскопії для високоточного розділення елементарних смуг в експериментальних спектрах фотолюмінесценції. Описано основні процедури аналізу та розрахунків у рамках цього методу. Метод випробувано на синтетичному спектрі фотолюмінесценції, що складається з п'яти елементарних гаусових смуг. Оцінено розділення нашого методу в застосуванні до гаусових смуг, які перекриваються, залежно від їхньої ширини. Проаналізовано спектр фотолюмінесценції нанокристалів ZnS:Mn, отриманих шляхом самопоширюваного високотемпературного синтезу, з використанням нашого методу похідної спектроскопії. Знайдено шість окремих смуг фотолюмінесценції, піки яких розташовані на довжинах хвиль 540, 559, 579, 600, 620 і 643 нм.